



## OPEN Genetic ancestry influences body shape and obesity risk in Latin American populations

Magda Alexandra Trujillo-Jiménez<sup>1,2,3</sup>✉, Luis Orlando Pérez<sup>1,3</sup>, Carolina Paschetta<sup>1,3</sup>, Virginia Ramallo<sup>1,3</sup>, Anahí Ruderman<sup>1,3</sup>, Mariana Useglio<sup>1,3</sup>, Pablo Toledo-Margalef<sup>1,3</sup>, Leonardo Morales<sup>1,3,13</sup>, Cindy Freire-Gómez<sup>1,3</sup>, Pablo Navarro<sup>1,3,13</sup>, Soledad De Azevedo<sup>1</sup>, Bruno Pazos<sup>1</sup>, Tamara Teodoroff<sup>1</sup>, Maria Cátira Bortolini<sup>6</sup>, Víctor Acuña-Alonzo<sup>7</sup>, Samuel Canizales-Quinteros<sup>8</sup>, Giovanni Poletti<sup>9</sup>, Carla Gallo<sup>9</sup>, Francisco Rothhammer<sup>10</sup>, Winston Rojas<sup>11</sup>, Andrés Ruiz-Linares<sup>12</sup>, Shanesia Gasaneo<sup>5</sup>, Gustavo Gasaneo<sup>5</sup>, Amanda Rowlands<sup>4</sup>, Pablo Nepomnaschy<sup>4</sup>, Claudio Delrieux<sup>2</sup> & Rolando Gonzalez-José<sup>1,3</sup>

Obesity is not simply a matter of excess weight. It also involves changes in structure and proportion in body morphology that can vary between populations and within individuals as they develop and age. Anthropometric measurements and their derived indices are widely used to study obesity. However, they present limitations to capture variations of fat distribution in the human body within a given population, and among different populations. Particularly, currently a problem in epidemiology is that cut-off points and health risk classifications based on anthropometric measures such as BMI, WHR or WHtR may not be equally valid for all population groups, especially when there are differences in genetic ancestry. Using data from ~ 7, 000 Latin American adults, we evaluated the accuracy of traditional indices across gradients of Native American, European, and African ancestry, and a comparison with three-dimensional (3D) body shape analysis, which offers a promising venue for capturing these complexities. We found that traditional indices systematically misclassified obesity-related risk in certain ancestry groups, with WHR and WHtR showing ancestry-specific biases. In contrast, 3D body shape promises to capture nuanced variations in fat distribution and reduced ancestry-related misclassification. By leveraging techniques based on advanced geometric morphometry and image and data processing, we can better characterize the interaction between genetic ancestry and body composition, ultimately improving the accuracy of obesity diagnosis and stratification in Latin American populations. These results highlight the need for ancestry-aware obesity diagnostics and demonstrate that integrating advanced 3D morphometric techniques can improve risk assessment and guide precision public health strategies in Latin America and beyond. We demonstrate that incorporating 3D body shape data alongside genetic ancestry data improves the accuracy of obesity risk stratification in Latin American populations. Our proposed methods could be adapted, expanded and applied to other populations.

**Keywords** Genetic ancestry, Admixed populations, Anthropometric indices, 3D body-shape

<sup>1</sup>Instituto Patagónico de Ciencias Sociales y Humanas, Centro Nacional Patagónico CCT CENPAT CONICET, Puerto Madryn U9120, Argentina. <sup>2</sup>Departamento de Ciencias e Ingeniería de la Computación, Universidad Nacional del Sur, B8000 Bahía Blanca, Argentina. <sup>3</sup>Programa de referencia y biobanco genómico de la población Argentina (PoblAr), Buenos Aires, Argentina. <sup>4</sup>Faculty of Health Sciences, Simon Fraser University, V5A 1S6 Burnaby, Canada. <sup>5</sup>Departamento de Física, Instituto de Física del Sur, Universidad Nacional del Sur, B8000 Bahía Blanca, Argentina. <sup>6</sup>Departamento de Genética, Instituto de Biociencias, Universidade Federal do Rio Grande do Sul, 91501-970 Porto Alegre, Brazil. <sup>7</sup>National Institute of Anthropology and History, 01030 Mexico City, Mexico. <sup>8</sup>Unidad de Genómica de Poblaciones Aplicada a la Salud, Facultad de Química, UNAM-Instituto Nacional de Medicina Genómica, 14610 Mexico City, Mexico. <sup>9</sup>Laboratorios de Investigación y Desarrollo, Facultad de Ciencias e Ingeniería, Universidad Peruana Cayetano Heredia, 150135 Lima, Peru. <sup>10</sup>Instituto de Alta Investigación, Universidad de Tarapacá, 7500531 Arica, Chile. <sup>11</sup>Grupo de Genética Molecular (GENMOL), Instituto de Biología, Universidad de Antioquia, 050010 Medellín, Colombia. <sup>12</sup>Ministry of Education Key Laboratory of Contemporary Anthropology, Collaborative Innovation Center of Genetics and Development, Fudan University, 200032 Shanghai, China. <sup>13</sup>Departamento de Informática, Universidad Nacional de la Patagonia San Juan Bosco, 9100 Trelew, Argentina. ✉email: ale.trujim@gmail.com

The global prevalence of obesity and its associated health concerns has been increasing dramatically over the last 50 years across human populations<sup>1</sup>. This increase in obesity prevalence may have its origins in emerging mismatches between past and present environments, particularly in current versus past energy availability and expenditure. Originally, *Homo sapiens communities*' sustenance depended exclusively from various combinations of ancestral hunting, gathering and, eventually, farming. Additionally, in ancestral populations parity was higher and individuals were exposed to higher risks of infection, predation or attacks by wildlife. Thus, energy availability was lower and energetic demands higher than those imposed by current industrial contexts. Within pre-industrial contexts, then, alleles associated with biological mechanisms that optimize energy efficiency and increase energy storage are hypothesized to have been advantageous and, thus, be positively selected<sup>2</sup>. Two main alternatives hypotheses have been proposed to explain these predispositions. The "Thrifty gene" hypothesis suggests that genes promoting efficient energy storage and fat accumulation were favored by natural selection because they improved survival during periods of food scarcity<sup>3</sup>. In contrast, the "Drifty gene" hypothesis proposes that, once predation pressures diminished in human evolutionary history, genetic drift allowed variation in appetite-regulating genes to accumulate, leading to increased susceptibility to obesity in modern environments<sup>3,4</sup>. Yet, in industrialized settings the same genetic predispositions and the biological mechanisms associated with them can increase the risk of developing phenotypes (observable physical characteristics) associated with obesity. The consequences of these mismatches are illustrated by the increase in obesity incidence in individuals who migrate from traditional agro-pastoral communities to urban, heavily industrialized contexts<sup>5</sup>.

Importantly, obesity is linked to increased risks of a broad range of health problems including diabetes, heart disease, mental health issues and negative reproductive outcomes<sup>6,7</sup>. Consequently, a number of anthropometric methods have been developed to detect and monitor obesity over the years. Traditional anthropometric indices to assess obesity include Body Mass Index (BMI), Waist-to-Hip Ratio (WHR), and Waist-to-Height Ratio (WHtR). While BMI reflects overall body mass relative to height, WHR and WHtR are widely used indicators of central fat distribution and abdominal obesity. These methods, however, have been criticized for not reflecting aspects of body composition that are critically important to accurately identify health risk profiles in diverse populations. In particular, evidence suggests that these indices may overestimate or underestimate health risks for some ancestry groups<sup>8–10</sup>, raising questions about their usefulness in regions with high genetic admixture<sup>11</sup>. Similar concerns have been discussed extensively in the literature since the introduction of BMI in 1974 by Ancel Keys<sup>12</sup>, and more recently in the context of body shape research<sup>13–16</sup>. These works emphasize that anthropometric indices, including body shape descriptors, have inherent methodological limitations and should be interpreted with caution<sup>11</sup>. These inaccuracies cannot only lead to ill-informed health policies but also, as a result, heighten health inequalities affecting historically marginalized groups with particular ancestries<sup>11</sup>. Human body morphologies vary occupying a continuous and multivariate space. This complexity can be driven by complex interactions between developmental, genetic, and environmental factors. Thus, understanding obesity and its health risks requires methodological approaches that capture meaningful variation in body size and shape. Nevertheless, current clinical assessments often rely on discrete thresholds and categorical classifications, such as BMI cutoffs, to estimate obesity-related risks, potentially overlooking the nuanced and continuous nature of body form variation. Regarding this, recently, Rubino et al. (2025) recommended that BMI should be used only as a surrogate measure of health risk at a population level, for epidemiological studies, or for screening purposes, rather than as an individual measure of health<sup>6</sup>.

The concerns described above have led to the development of novel ways to study and assess obesity in different populations across time and space. New diagnostics tools include new technologies including 3D scanning, video-based models and image processing, which are illustrated in Fig. 1. Traditional and widespread ways of detecting overweight and obesity were based on anthropometric measurements combined on several indices that, as a norm, provide an easy and accessible way to approach in a statistical way the study of the phenotype of interest. Yet, the obesity phenotype is an intrinsically complex one, particularly in terms of the variety of patterns in which fat can be distributed in the human body. Proper assessment of such patterns requires capturing a variety of 3D geometric profiles. Gold-standard imaging techniques such as computed tomography (CT) and magnetic resonance imaging (MRI) have been extensively used to assess obesity phenotypes<sup>17–19</sup>. These modalities allow precise quantification of adipose tissue distribution, differentiation between visceral and subcutaneous fat compartments, and evaluation of ectopic fat deposition, all of which are strongly associated with metabolic risk<sup>19</sup>. Studies employing CT and MRI have demonstrated that central fat accumulation, rather than total body fat alone, is a stronger predictor of cardiometabolic disease<sup>20</sup>. While their high cost and limited accessibility in large, population-based studies constrain their widespread application, they remain critical benchmarks against which newer, more scalable approaches, such as 3D body surface scanning, can be validated. To that effect it is necessary to utilize 3D devices and statistical models that can accommodate this type of data. Attaining a proper, comprehensive and accurate evaluation of the obesity phenotype, is critical to achieving greater refinement in its study, needed to complement precision strategies at other population structure levels (genomic, epigenomic, etc). It is important to note, however, that principal component analysis PCA-based body shape phenotyping, while capturing variation beyond traditional indices, also faces constraints regarding resolution, interpretability, and clinical applicability<sup>13,15,16</sup>. As highlighted by the 2024 Lancet Obesity Commission, the current challenge in obesity research lies in refining its conceptual and clinical definition, rather than relying solely on anthropometric or morphometric phenotyping<sup>21</sup>.

Latin America, with its rich history of biological and cultural admixture, is an example of a region likely to be affected by the misclassification of obesity phenotypes. The sub-continent underwent extensive admixture between Native Americans and people arriving from other continents, particularly Europe and Africa<sup>22–25</sup>. Most genetic studies have examined this process using a "tri-hybrid" model that includes variation in overall Native American, European and Sub-Saharan African ancestry across regions and amongst individuals<sup>23–25</sup>, with small and geographically-restricted East Asian ancestry also reported<sup>26</sup>. Recent research using novel haplotype-based

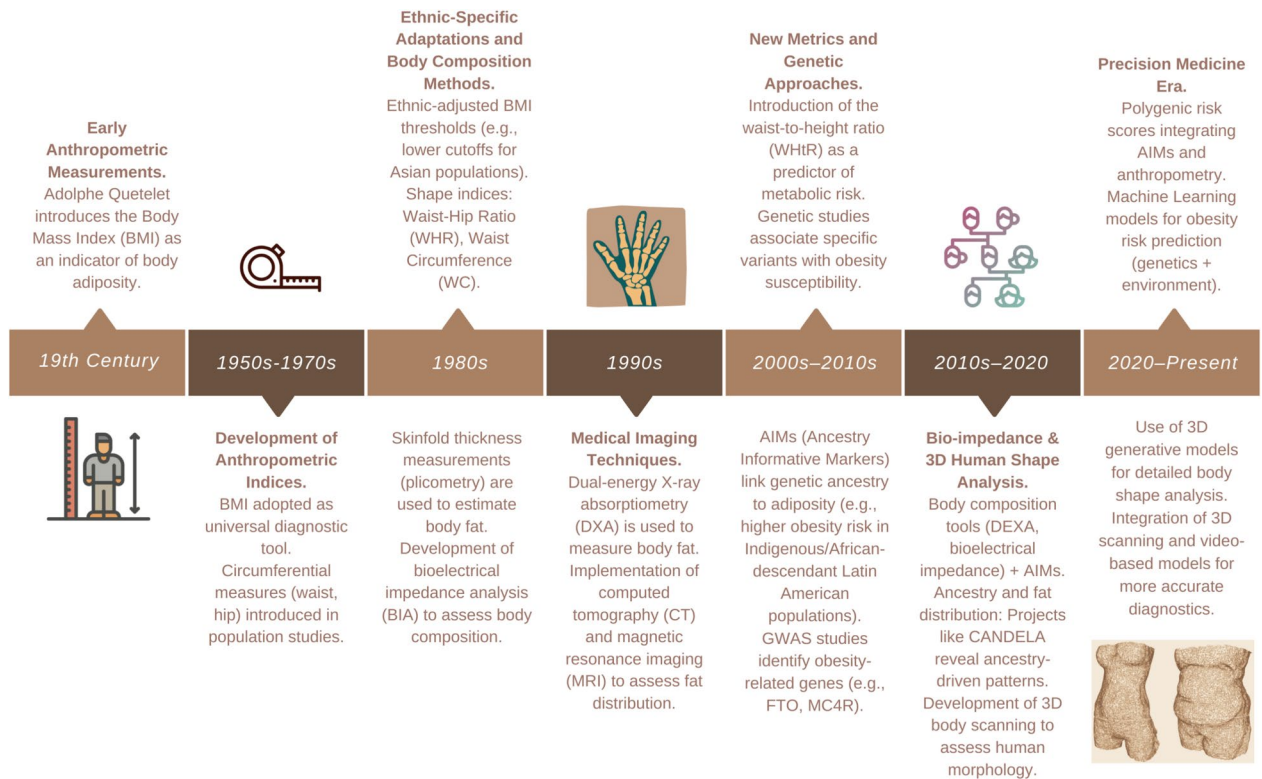


**Fig. 1.** Evolution of methods to study overweight and obesity, and the role of genetic ancestry.

methods, showed that Native American ancestry components in Latin Americans correspond geographically to the present-day genetic structure of Native groups, and that sources of non-Native ancestry, and admixture timings, match documented migratory flows<sup>25</sup>. As a whole, these and other studies help to document a fine-grained landscape of genetic and non-genetic factors that arose after five centuries of extensive admixture and migratory movements in the region.

The Latin American fine-grained admixture dynamics described above represents a fruitful scenario to detect genetic markers associated to phenotypes via admixture mapping approaches. Indeed, the CANDELA initiative has investigated samples from Latin American admixed populations to help verify the presence of previously reported genetic markers, including Single Nucleotide Polymorphisms (SNPs), and to report new markers associated to several phenotypes such as facial shape<sup>27</sup>, eyebrow shape<sup>28</sup>, skin and/or hair pigmentation, dental size and shape<sup>29</sup>, pain sensitivity<sup>30</sup>, cancer risk<sup>31,32</sup>, ear morphology<sup>27</sup>, and geometric-morphometric obesity-related traits<sup>33-36</sup>. These examples, along with other research published elsewhere on admixed groups<sup>5,22,37-39</sup> demonstrate that complex traits do present ancestry-driven patterns that are likely to result in diverse metabolic profiles.

Our goal is to take advantage of well-known Latin American admixture dynamics to assess whether traditional indices are appropriate to accurately identify obesity and health risk across populations. Our results should help inform public health strategies in Latin America that are specific to each country's population structure. Here, we test the hypothesis that obesity classifications based on traditional anthropometric indices present discrepancies across genetic ancestry groups, which renders universal diagnostic criteria for obesity-associated health risks inappropriate. To this aim, we investigate the links between traditional anthropometric indices associated with obesity, genetic ancestry and health risks. Finally, we propose the development of new methodological approaches that go beyond traditional indices and incorporate a deeper understanding of body shape variation, acknowledging that such phenotyping is complementary to, rather than a substitute for, comprehensive clinical stratification frameworks<sup>21</sup>.

## Methods

### Data integration and preprocessing

We integrated five (5) databases containing anthropometric indices, Ancestry-Informative Markers (AIMs), and/or 3D body shape to assess the influence of genetic ancestry on body shape and obesity risk from a total of seven (7) countries. Specifically, we analyzed data from the CANDELA consortium (Colombia, Mexico, Chile, Brazil, Peru), as well as from three projects in Argentina: *Raíces*, *Patagonia3D*Lab, and *ECHA* (Emoción, Cognición y Hábitos Alimentarios), and the *SER project* (Society, Environment, and Reproduction Research) based in Guatemala. All the databases contain the anthropometric indices on which our analyses are based: Body Mass Index (BMI), Waist-Hip Ratio (WHR), and Waist-to-Height Ratio (WHtR)<sup>35,40-44</sup>. All studies but *SER* included Genetic Ancestry-Informative Markers. That said, *SER* participants' indigenous ancestry is well established,

allowing us to classify them safely within the America AIM category<sup>45</sup>. Inclusion criteria for participants were adults older than 18 years, availability of complete anthropometric and genetic ancestry data, and absence of conditions affecting body composition such as pregnancy or severe musculoskeletal disorders. Sample sizes per site are provided in Table 1.

### Database descriptions

**CANDELA Consortium<sup>40</sup>:** This large-scale study, which included 7,235 participants collected in 2012, was designed to investigate genetic and environmental influences on physical and facial traits. This database includes individuals of both sexes from five (5) cities in five (5) Latin American countries: Porto Alegre in Brazil; Arica in Chile, Medellín in Colombia; Mexico City in Mexico; and Lima in Peru. Further details regarding the *CANDELA consortium* (<http://www.ucl.ac.uk/silva/candela>) study can be found in Ruiz-Linares et al. (2014). The *CANDELA consortium* project obtained its own ethical clearance from the University College London (UK, protocol number 3352/001), and was approved by all participating institutions: Universidad Nacional Autónoma de México (México), Universidad de Antioquia (Colombia), Universidad Peruana Cayetano Heredia (Perú), Universidad de Tarapacá (Chile), Universidade Federal do Rio Grande do Sul (Brazil) and University College London (UK). Informed consent was obtained from all participants.

**Raíces<sup>41</sup>, Patagonia3D Lab<sup>35</sup>, and ECHA<sup>42</sup>:** These projects investigate anthropometric and morphological diversity in Argentine populations<sup>43</sup>. Data collection took place in: 2018 for *Raíces*, 2016 for *Patagonia3D Lab*, and 2022 for *ECHA*. They all include anthropometric indices and *Raíces* also includes 3D body models and AIM data in 96 individuals. The *Raíces* project was approved by the Research Ethics Committee of the Northern Programmatic Area of the Ministry of Health of the province of Chubut (Regional Hospital of Puerto Madryn, Chubut, Argentina) under protocol number 19/17 (approved on September 4, 2017). The *Patagonia 3D Lab* project, prior to *Raíces*, was approved by the same Ethics Committee under protocol number 010/16 (approved on June 9, 2016).

**SER project<sup>44</sup>:** *SER* is a longitudinal project that began in 2000 to examine the interactions between society, environment, and reproduction in a Maya-Kachikel population from Guatemala. For the analyses in this article we included anthropometric data including BMI, WHR and WHtR and 3D data collected in 2023. *SER*'s data collection and use was approved by the Research Ethics Board (REB) at Simon Fraser University (SFU) (Application Numbers: 2012s0668 and 2016s0576).

The total sample size of these five datasets provides a final sample of 7,757 individuals (of both sexes, except for the Guatemala sample, which contains only females) from seven Latin American countries: Colombia, Mexico, Chile, Brazil, Peru, Argentina, and Guatemala.

### Genetic ancestry: definition and estimation

Genetic ancestry measures the genetic variation in DNA to assess the geographical origins of individuals' ancestors<sup>46</sup>. Genetic ancestry is a multidimensional continuum that can, for example, reflect the proportion of an individual's ancestry originating from Africa, the Americas, Asia or Europe at a continental level, and can also be assessed using finer scales (e.g. Chacón-Duque et al. 2018<sup>25</sup>)<sup>46–49</sup>. In contrast to race and ethnicity, genetic ancestry is directly linked to genetic variation, which in turn may be related to particular biological processes<sup>47,49</sup>. As such, genetic ancestry captures a portion of the biological variation between and within groups.

Despite the continuous and multifactorial nature of genetic ancestry, we rely on broad categorical groupings in this study because they offer a practical and reproducible way to summarize complex genetic information. These groupings, such as individuals with predominantly Amerindian, European, or African ancestry, serve as useful proxies to identify general trends. However, we acknowledge that these categories are simplifications of a much richer underlying variation. Future approaches that incorporate ancestry as a continuous variable or explore ancestry at more local levels using specific genomic regions may provide even more precise insights into how genetic background shapes human morphology and metabolic health.

The concept of ancestry can be defined as a description of a person's origin from his or her genetic lineage. However, its use in scientific research and public discourse has generated debates about its meaning and implications. The confusion between genetic ancestry, race and ethnicity has led to misinterpretations and problematic use of these categories in fields such as medicine and anthropology. Race and ethnicity are social

Country	Dataset(s)	Collection year	Sample Size (female/male)	Mean Weight/ WC / HC	3D Body Models	AIMs Available	Ancestry Estimation Method
Brazil	CANDELA <sup>40</sup>	2014	1045 / 499	67.4 / 80.8 / 100.4	No	Yes	Direct estimation based on AIMs
Chile	CANDELA <sup>40</sup>	2014	518 / 1035	72.7 / 86.4 / 101.7	No	Yes	Direct estimation based on AIMs
Colombia	CANDELA <sup>40</sup>	2014	926 / 721	63.7 / 79.6 / 95.6	No	Yes	Direct estimation based on AIMs
México	CANDELA <sup>40</sup>	2014	954 / 632	72.9 / 92.2 / 106.3	No	Yes	Direct estimation based on AIMs
Perú	CANDELA <sup>40</sup>	2014	545 / 360	64.8 / 84.2 / 97.6	No	Yes	Direct estimation based on AIMs
Argentina	Patagonia3D Lab <sup>35</sup> Raíces <sup>41</sup> ECHA <sup>42</sup>	2016 2018 2023	112 / 42 100 / 45 80 / 26	72.3 / 90.5 / 102.9	Yes (Raíces only, N=96)	Yes	Direct estimation based on AIMs
Guatemala	SER <sup>44</sup> (2023 update)	2024	116 / 0	58.4 / 90.4 / 100.3	Yes	No	Assumed Native American ancestry based on documented demographic history <sup>45</sup>

**Table 1.** Summary of integrated datasets by country, detailing available data types and ancestry estimation methods, and mean values for Weight, WC (Waist Circumference), and HC (Hip Circumference).

constructs influenced by historical, political, and cultural factors, whereas genetic ancestry is based on DNA variability and allows estimating the geographic origin of a person's ancestors<sup>47</sup>. This approach has limitations, as genetic diversity is a continuum without fixed boundaries, and categorizing populations based on genetics alone can lead to misinterpretations. While genetic ancestry can provide relevant information in biomedical studies, it should not be used as a proxy for race or ethnicity, as these categories reflect social experiences that impact health and life chances. Ignoring this dimension may reinforce biological determinism and generate biased conclusions<sup>49</sup>. Therefore, it is crucial to employ these concepts accurately, recognizing both their differences and their interactions.

To accurately characterize population structure, it is essential to define ancestry and the genetic markers used for its estimation. Continuing in the line of genetic ancestry, Ancestry-Informative Markers (AIMs) are genetic variants specifically selected for their ability to differentiate ancestral populations through allele frequency differences across geographical groups. In the datasets analyzed here, AIMs correspond to *Single Nucleotide Polymorphisms (SNPs)*, as used in the CANDELA study and related initiatives<sup>40,50,51</sup>. In admixed populations, such as those in Latin America, AIMs allow for the estimation of ancestry proportions, reducing potential bias due to population structure, a well-known confounding factor in association studies. Based on these SNP markers, individuals can be characterized by their proportion of major continental ancestries (commonly African, European, and Amerindian), enabling the exploration of how genetic ancestry relates to phenotypic variation.

In this sense, Latin America's admixed populations exemplify the complex interplay of genetic ancestry, environment, and culture in shaping obesity phenotypes. By combining AIM-based genomics with 3D morphometrics, we move beyond the limitations of traditional anthropometry toward precision public health. The approach used here highlights several aspects of interest regarding the biological and non-biological causes of obesity. It should be noted that the exploration of new approaches to study obesity, overcoming the limitations of traditional anthropometric indices, has clinical relevance since it aims to address diagnostic gaps existing in real-world settings.

### Anthropometric indices and risk classification across ancestry groups

Individuals at high-risk of metabolic and cardiovascular diseases were identified using categorical thresholds based solely on anthropometric indices using WHO criteria based on obesity risks<sup>52</sup>. Although ethnicity-specific BMI and WHR cut-off values have been proposed<sup>53</sup>, we applied WHO thresholds to ensure consistency and comparability of classifications across the multi-country, genetically diverse sample analyzed in this study. For BMI, individuals were categorized as “Overweight” (BMI 25.0–29.9), “Obesity class I” (30.0–34.9), “Obesity class II” (35.0–39.9), and “Obesity class III” ( $\geq 40.0$ ), reflecting increasing severity of obesity-related health risks. The categories “Underweight” (BMI  $<18.5$ ) and “Normal weight” (BMI 18.5–24.9) were not considered obesity high-risk. WHR risk thresholds were set at  $>0.85$  for women and  $>0.90$  for men, indicating increased risk for cardiometabolic diseases<sup>54,55</sup>. For WHtR, a cut-off of  $>0.50$  was used, which has been widely associated with elevated risk for central adiposity and metabolic syndrome<sup>54</sup>. These classifications are regularly used to identify at-risk individuals across populations, and to evaluate health disparities within and between genetically admixed groups. This analysis was carried out both at the country level and within each country, stratifying the data by AIM groups.

To assess whether the distributions of anthropometric indices varied across genetic ancestry groups, we applied the non-parametric Kruskal–Wallis test separately for male and female participants. This test is suitable for comparing the distribution of ranks across three or more independent groups when the assumption of normality is not met. It is used to assess whether the groups originate from the same distribution and is appropriate when the grouping variable is categorical, as is the case for ancestry categories<sup>56</sup>. *Post hoc* pairwise comparisons were conducted using Dunn's test, with Bonferroni correction to account for multiple testing<sup>57</sup>. This analysis was applied to BMI, WHR, and WHtR. Additionally, we recoded each anthropometric index into binary risk categories (low vs. high disease risk) and performed chi-square tests of independence on contingency tables stratified by sex to test whether the application of current diagnostic thresholds leads to unequal classification of risk across ancestry groups. For WHR and WHtR, we maintained our standard binary cut-offs, whereas for BMI we grouped “Underweight” and “Normal weight” into a “low-risk” category, and combined “Overweight” and all obesity classes (I–III) into a “high-risk” group.

Additionally, the Body Shape Index (ABSI) and the Hip Mass Index (HI), two more recent ones that offer a complementary perspective on disease risk, were calculated. The ABSI, developed to be independent of weight and height, has been associated with all-cause and cardiovascular disease mortality in various population-based studies<sup>58,59</sup>. On the other hand, the HI, which assesses hip mass, has also shown associations with adverse health outcomes<sup>60,61</sup>.

### Descriptive analysis by country and by ancestry-informative marker

Subsequently, individuals were reclassified based on their genetic ancestry using AIMs. We used an arbitrary threshold of  $>70\%$  of per-individual AIMs belonging to each parental population to maximize the chances of detecting ancestry-dependent anthropometric variation<sup>62</sup>. As a result of this reclassification, a subset of 2,970 individuals (1,878 females and 1,092 males) was identified as having predominantly Native American, European, or African ancestry (see Fig. 2). These three groups represent distinct genetic profiles derived from the commonly used tri-hybrid model (America, Europe, Africa). It is important to clarify here that we are not assuming that our sample can be dissected into three continental groups, which do not represent biological entities per se. Rather, we just simply implement a rotation of the AIMs' statistical space in order to maximize the anthropometric variation potentially due to differences in genetic ancestry.

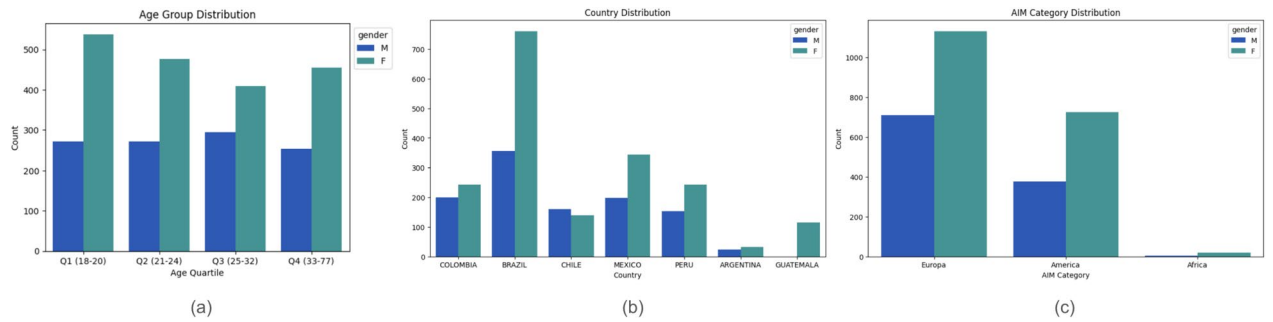


**Fig. 2.** Sample distribution across age groups, countries, and ancestry-informative markers (AIM) categories, stratified by sex. **(a)** Age quartile distribution of the sample, showing differences in the number of individuals per age group and sex. **(b)** Country-wise distribution of the dataset after AIM filtering, highlighting the relative representation of each country. **(c)** Distribution of individuals according to their predominant AIM category (Europe, America, or Africa), considering only those with at least 70% ancestry membership.

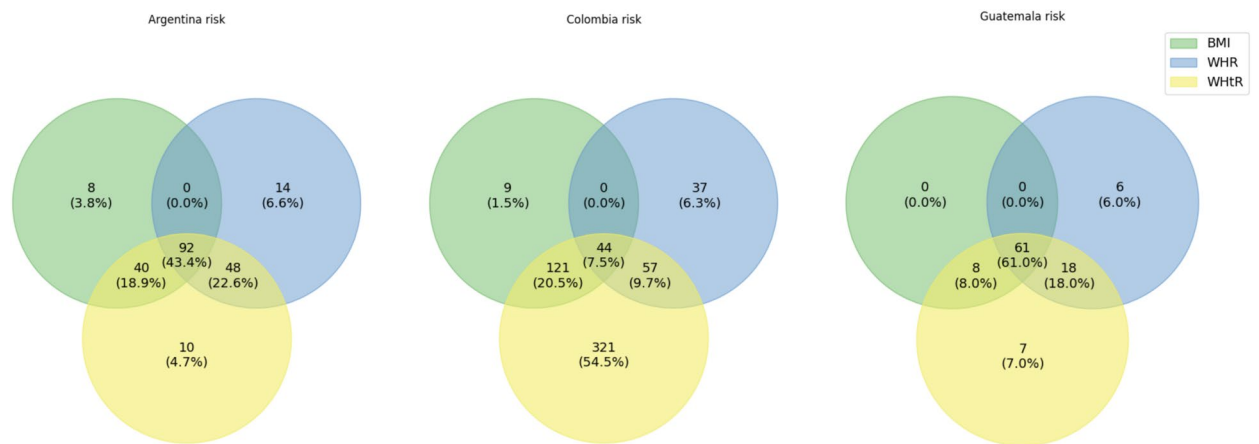


**Fig. 3.** Sample of Venn diagrams used to visualize the overlap of individuals classified as high-risk according to BMI, WHR, and WHtR thresholds.

To explore disparities in risk classification, we constructed Venn diagrams to visualize the overlap of high-risk participants identified by different anthropometric indices (BMI, WHR and WHtR) across countries and AIM categories (Europe, America & Africa) (see Fig. 3). These visualizations provided insight into the extent of agreement or divergence among classification methods. Additionally, statistical comparisons were performed using the Kruskal-Wallis test to determine whether significant differences existed in the distribution of anthropometric indices across groups. These steps were crucial for assessing the degree of consistency or disparity in risk categorization across traditional anthropometric measures.

We conducted a Principal Component Analysis (PCA) to examine the underlying structure of individuals' anthropometric data, and to explore the position of individuals according to their anthropometric indices' threshold and or their genetic ancestry. Our objective was to identify the Eigenvectors (Principal Components) that best explain the variance in the data. We then visualized the PCA results to explore clustering patterns and assess the influence of ancestry on body shape variation. We applied all analyses separately for male and female sub-samples to account for sex-based differences in body shape and disease risk classification. This comprehensive analytical approach enabled us to robustly evaluate inter-country and inter-ancestry variation in body shape, revealing patterns beyond geopolitical borders. These PCA analyses were conducted using the PCA module from the Scikit-learn library (version 1.6.1)<sup>63</sup> in Python 3.11.13.

### 3D human shape variation

To analyze body shape variation, we obtained 3D models from two sources: direct 3D scans and video-based reconstructions. High-resolution 3D scans were acquired using the Structure Sensor scanner for a subset of individuals from the Raíces and Patagonia3D Lab databases<sup>43,64</sup>. Additionally, 3D body reconstructions were generated from video recordings using the *body2vec\_mesh* model ([https://github.com/aletrujim/body2vec\\_mesh](https://github.com/aletrujim/body2vec_mesh)), which integrates multiple Deep Learning approaches: background removal with BremNet<sup>36</sup>, pose estimation with OpenPose<sup>65</sup>, and 3D human body generation based on PIFuHD<sup>66</sup>. The ECHA and SER databases included only the video-based reconstructions, without direct 3D scans.

To ensure comparability across datasets, all 3D models were aligned, rotated, and scaled using Procrustes analysis within each database. Procrustes analysis is a geometric method used to standardize 3D shapes by removing differences in position, rotation, and scale while preserving the intrinsic shape variation<sup>67</sup>. This technique aligns all models to a common reference framework, ensuring that differences observed across individuals are due to actual morphological variation rather than differences in orientation or size<sup>68</sup>. By applying Procrustes superimposition to our dataset, we were able to compare body shape variation across individuals and populations in a standardized way, facilitating subsequent statistical analyses of shape differences. The patterns of variation in body shape were then explored through PCA, which allowed the identification of the main axes of morphological differences between individuals. These analyses were performed using the SciPy library (version 1.15.3)<sup>69</sup> and Open3D library (version 0.19.0)<sup>70</sup> in Python 3.11.13.

## Results

Significant differences were found across all three anthropometric indices (BMI, WHR, WHtR) among genetic ancestry groups, indicating systematic variation in body composition (see Fig. 4). Differences were most pronounced for WHR and WHtR, which showed higher Kruskal–Wallis statistics than BMI, suggesting that these fat distribution measures are more sensitive to ancestry-related variation (see Table 2). Among females, Native American ancestry was associated with significantly higher BMI compared to African and European groups, which did not differ significantly from each other. WHR and WHtR differed significantly across all ancestry groups, with Native American women exhibiting the highest values, followed by Europeans and Africans. In males, Native Americans also had the highest values for all indices, followed by Europeans and Africans, with significant differences observed between African and European men across all measures, including BMI.

*Post hoc* Dunn tests revealed significant differences between all three ancestry groups, with the differences between African and European males being the least pronounced (see Table 3). In general, WHR emerged as the most discriminative index between ancestry groups, showing consistently strong differences. These results highlight the importance of accounting for ancestry when interpreting anthropometric measures and assessing cardiometabolic risk. Overall, the distribution of BMI, WHR, and WHtR varies significantly by ancestry, indicating that applying uniform diagnostic thresholds across populations may lead to misclassification—overestimating risk in some groups and underestimating in others. Differences in risk classification are shaped not only by health variation, but also by how risk is measured and where thresholds are drawn. This points to a potential structural bias, as current thresholds do not reflect population-specific body composition patterns. Notably, individuals with Native American ancestry were consistently classified at higher risk across all indices and sexes, underscoring the need for ancestry-adjusted criteria to improve equity and accuracy in risk assessment).

Additional analyses including waist circumference (WC) showed significant differences across ancestry groups in both sexes ( $p < 0.001$ , Kruskal–Wallis). However, effect sizes were consistently greater for WHR and WHtR than for WC and BMI.

Chi-square tests conducted on contingency tables of risk categories by ancestry group and sex revealed statistically significant differences across all anthropometric indices (see Table 2). These results indicate that the current diagnostic thresholds produce unequal classifications of cardiometabolic risk across ancestry groups. Figure 5 illustrates marked disparities in the proportion of individuals classified as “at risk” with consistently higher prevalence among those with predominantly Native American ancestry across nearly all indices and both sexes. While the magnitude of these differences varies by index, the overall pattern persists, suggesting that the issue cannot be solely attributed to the technical properties of a given index. Rather, it reflects a potential structural diagnostic bias arising from the use of cut-off points that have not been calibrated to diverse body phenotypes. If existing criteria could be reliably applicable across populations, the proportion of individuals classified as high risk would reflect true underlying health disparities rather than artifacts of measurement. While it is acknowledged that disease burden is not necessarily distributed homogeneously across populations, the consistent and pronounced over and under representation of certain ancestry groups in high-risk categories suggests that current thresholds may not adequately account for the variation in ancestry-specific body composition patterns among populations. Thus, the observed disparities likely reflect a combination of true epidemiological differences and structural biases in diagnostic criteria.

Considering the analysis by country and information marker of ancestry (using a >70% ancestry membership threshold), our results suggest that the health risk profile varied more in our sample amongst individuals with predominant European ancestry. This sub-sample also had a higher concentration of high-risk individuals in terms of BMI than other groups. We also observed that the American ancestry predominant sub-sample displayed a high prevalence of risk across all anthropometric indices, with a substantial overlap in high-risk categories for WHR and WHtR, with 26.7% (female) and 38.0% (male) of individuals in this group simultaneously exceeding the risk thresholds for both indices. This prevalence was notably higher than that observed in the European and African predominant ancestry groups, highlighting a distinct pattern of central adiposity-related risk within this population.

The Kruskal–Wallis test revealed significant differences in anthropometric indices (BMI, WHR, WHtR) across AIM categories in both female and male populations (see Table 4). Our results show that in females body shape variation is influenced by genetic ancestry when considering highly informative AIM classifications ( $H = 9.66$ ,  $p = 0.008$ ). Consistent with our hypothesis we also observed differences among male AIM groups ( $H = 8.88$ ,  $p = 0.012$ ).

Unlike our finding with AIMS, the distribution of anthropometric indices did not vary amongst countries for either sex. The Kruskal–Wallis test for females ( $H = 7.32$ ,  $p = 0.292$ ) and males ( $H = 4.97$ ,  $p = 0.420$ ) suggested that body shape variation does not significantly differ between national populations. These findings contrast with the AIM-based analysis, emphasizing that genetic ancestry rather than geopolitical borders may play a more substantial role in anthropometric variation.

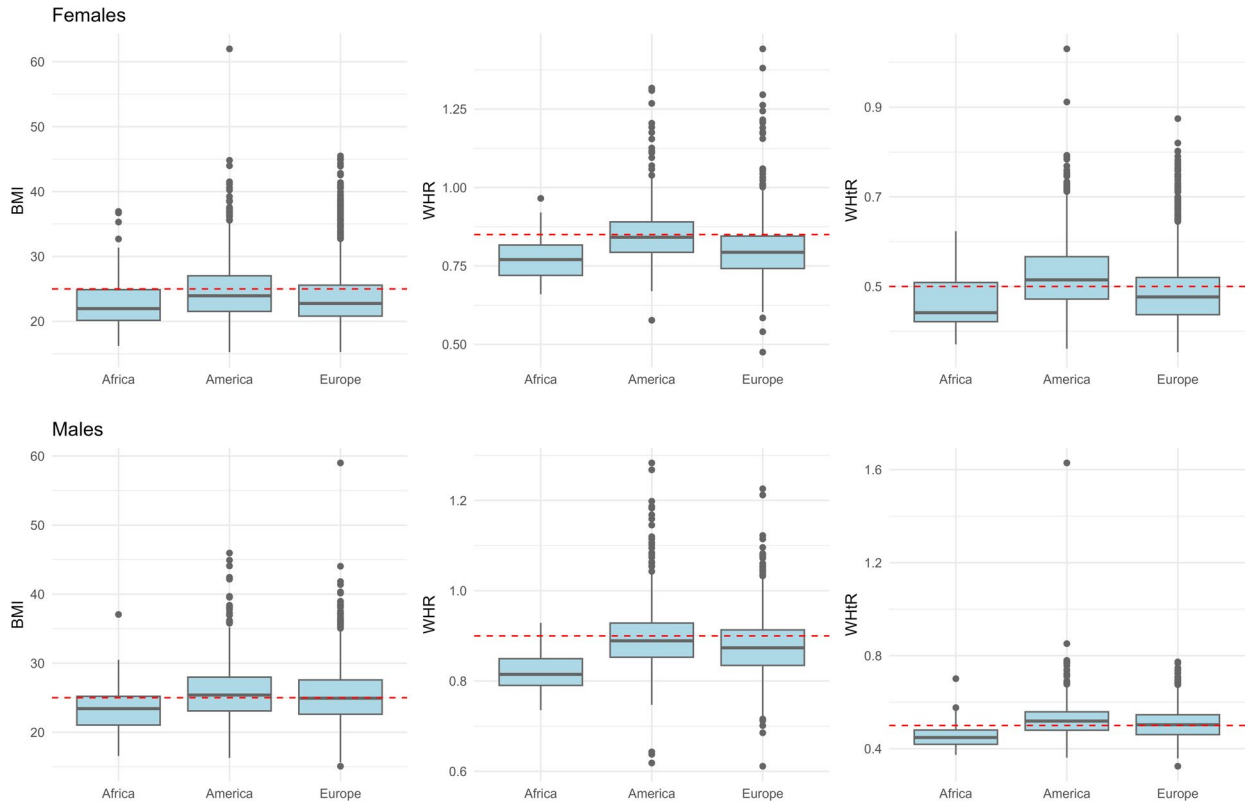


**Fig. 4.** Distribution of anthropometric indices by ancestry group, stratified by sex. Boxplots represent the distribution of values for each anthropometric index across ancestry groups (African, American, and European). Dashed red lines indicate the current cutoff points recommended by the World Health Organization<sup>52</sup> for identifying increased health risk.

Index	H Value K-W	p-value K-W	Chi-squared $\chi^2$	p-value $\chi^2$
BMI (Females)	63.16	0.00000	48.63	$2.75 \times 10^{-11}$
BMI (Males)	18.08	0.00012	15.46	0.0004383
WHR (Females)	329.32	0.00000	195.94	$2.2 \times 10^{-16}$
WHR (Males)	81.17	0.00000	41.34	$1.05 \times 10^{-9}$
WHtR (Females)	278.44	0.00000	191.19	$2.2 \times 10^{-16}$
WHtR (Males)	64.78	0.00000	47.07	$6.02 \times 10^{-11}$

**Table 2.** Summary of Kruskal–Wallis and Pearson Chi-squared test results for differences across genetic ancestry groups in each anthropometric index, stratified by sex. Both tests show consistent statistically significant differences across ancestry groups.

The ABSI and HI anthropometric indices were calculated for all participants. For the ABSI, the mean was 0.077599 ( $\pm 0.005284$ ), consistent with the average values ( $\sim 0.078$ ) reported in Krakauer’s original studies (2012). The HI had a mean of 0.180953 ( $\pm 0.007604$ ), an acceptable value given its range is similar to that of the ABSI. As expected, strong positive correlations were observed between traditional central adiposity metrics. For example, BMI showed a very high correlation with WC ( $r = 0.82$ ) and HC ( $r = 0.83$ ). Similarly, WHtR showed an extremely high correlation with WC ( $r = 0.90$ ) and HC ( $r = 0.74$ ), confirming its usefulness as a robust indicator of central adiposity. As expected, the correlation matrix also validates the statistical independence of ABSI and HI with respect to height and BMI. The correlation of ABSI with height ( $r = -0.08$ ) and BMI ( $r = -0.01$ ) was close to zero. Similarly, the correlation of HI with height ( $r = -0.01$ ) and BMI ( $r = -0.18$ ) was also very low. These findings suggest that ABSI and HI are unique measures that are not redundant with more common metrics, justifying their inclusion as complementary indicators in risk analysis.

Our PCA analysis of the BMI, WHR and WHtR anthropometric indices shows that the first two principal components explain most of the variance in both female and male groups (see Fig. 6). In the female group, the first principal component (PC1) explains approximately 80.77% of the variance, while the second principal

Index	Score	Africa-America	Africa-Europe	America-Europe
BMI (Females)	Z	-4.08	-1.83	7.45
	P.unadj	0.00005	0.06776	0.00000
	P.adj	0.00014	0.20329	0.00000
BMI (Males)	Z	-3.22	-2.49	3.20
	P.unadj	0.00128	0.01280	0.00136
	P.adj	0.00383	0.03839	0.00409
WHR (Females)	Z	-7.81	-2.50	17.53
	P.unadj	0.00000	0.01231	0.00000
	P.adj	0.00000	0.03692	0.00000
WHR (Males)	Z	-6.81	-5.26	6.79
	P.unadj	0.00000	0.00000	0.00000
	P.adj	0.00000	0.00000	0.00000
WHtR (Females)	Z	-7.74	-2.92	15.94
	P.unadj	0.00000	0.00352	0.00000
	P.adj	0.00000	0.01057	0.00000
WHtR (Males)	Z	-5.87	-4.43	6.28
	P.unadj	0.00000	0.00001	0.00000
	P.adj	0.00000	0.00003	0.00000

**Table 3.** Post hoc Dunn test results for pairwise comparisons of ancestry groups (Africa, America, Europe) across anthropometric indices, stratified by sex. The table reports Z-scores, unadjusted p-values (P.unadj), and Bonferroni-adjusted p-values (P.adj). All indices show statistically significant differences between most ancestry pairs, with the most pronounced differences observed in comparisons involving the American group.

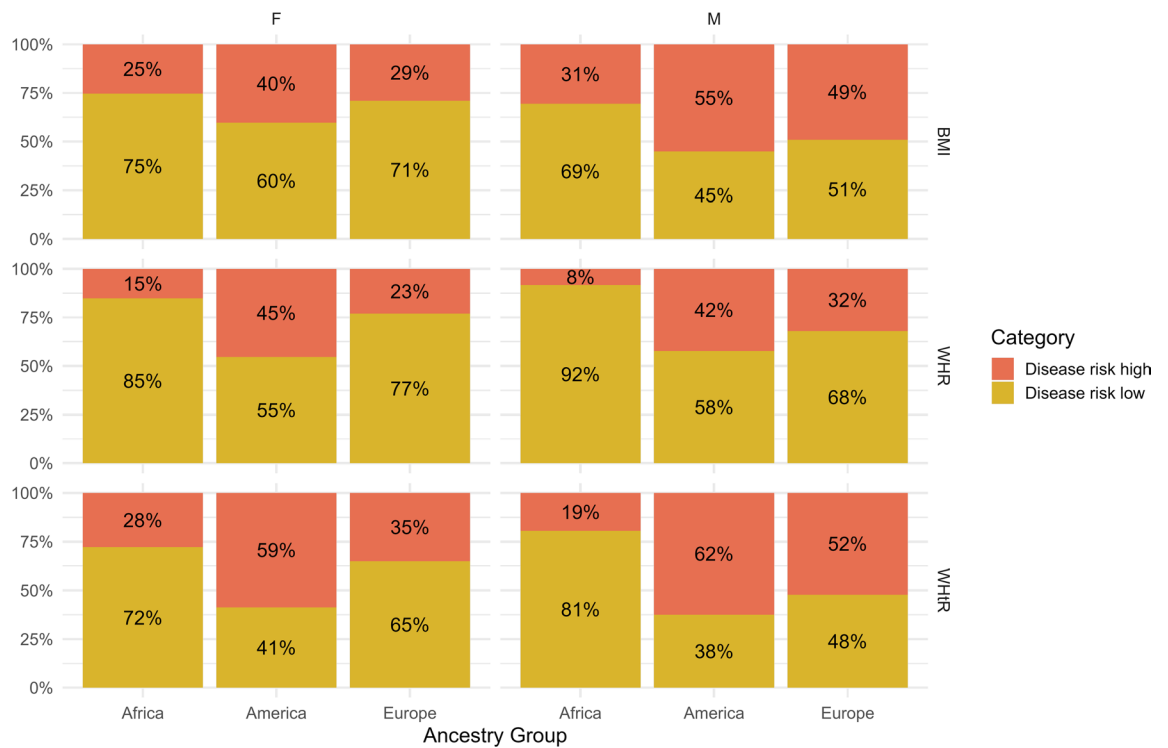


**Fig. 5.** Proportional risk distribution across indices and sex.

component (PC2) explains 17.85%. For the male group, PC1 explains 83.10% of the variance and PC2 explains 12.46%. In terms of the eigenvectors, in both groups PC1 is dominated by similar contributions from the three anthropometric indices, with slightly different values: in female, BMI (0.5571), WHR (0.5362) and WHtR (0.6341), while in male, BMI (0.5675), WHR (0.5576) and WHtR (0.6058). This suggests that this component captures a combination of the three measures as a general pattern of body variation. On the other hand, PC2 presents negative values for BMI and WHtR, and positive values for WHR in both groups. In females, the values

Comparison	H Value	p-value	Significance	Findings
AIM groups (Females)	9.66	0.008	Significant	Body shape variation is influenced by genetic ancestry in females with highly informative AIM classifications.
AIM groups (Males)	8.88	0.012	Significant	Differences were observed among male AIM groups, supporting the hypothesis of ancestry-driven variation.
Countries (Females)	7.32	0.292	Not significant	No significant variation in body shape among national populations in females.
Countries (Males)	4.97	0.420	Not significant	No significant variation in body shape among national populations in males.

**Table 4.** Summary of Kruskal-Wallis test results for anthropometric indices across ancestry-informative marker (AIM) groups and national populations, separately for females and males.

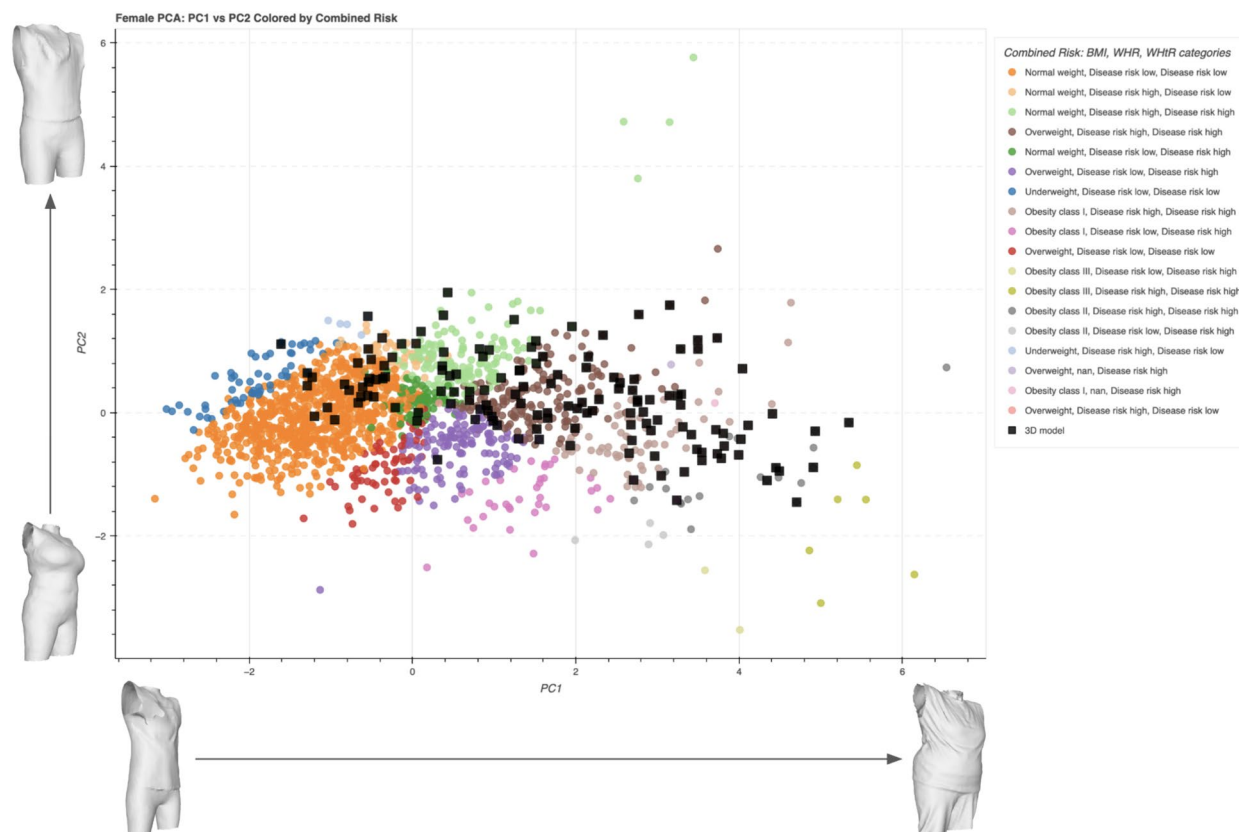


**Fig. 6.** Principal Component Analysis (PCA) of female colored by combined risk categories derived from BMI, WHR, and WHtR. Each point represents an individual, with colors indicating combinations of obesity classifications and associated disease risk levels according to WHO criteria. Black squares represent the subset of individuals with available 3D models, whose extreme body shapes are shown along the PCA axes.

are BMI (-0.6662), WHR (0.7444) and WHtR (-0.0441), while in male they are BMI (-0.6662), WHR (0.7434) and WHtR (-0.0602). This indicates that the second principal component mainly differentiates between BMI and WHR, with a smaller impact of WHtR. Overall, these results suggest that the relationships between BMI, WHR and WHtR are similar in both sexes, albeit with small differences in the proportion of variance explained and in the weights of the variables in the principal components.

Figure 7 presents the distribution of the first principal component (PC1) from the principal component analysis (PCA) among female participants, stratified (colored) by combined risk categories derived from BMI, WHR, and WHtR indicators. A clear upward trend in PC1 values is observed across increasing risk levels, with the lowest scores found in women classified as underweight or normal weight with low disease risk, and the highest scores in those classified as “Obesity class III” with high disease risk. This pattern suggests that PC1 captures morphological variations related to increased body mass and central fat accumulation, highlighting a shape-based gradient associated with cardiometabolic risk.

The effect of Generalized Procrustes Analysis (GPA) on 3D body model alignment is illustrated in Fig. 8. The left panel depicts the unaligned configurations, where each point cloud corresponds to a distinct model. Significant variability in position, scale, and orientation is observed, hindering direct shape comparison. In contrast, the right panel presents the models after Procrustes alignment to a common reference (highlighted in red). This process eliminates differences attributable to translation, rotation, and scaling, facilitating a precise

assessment of shape variation. The convergence of the point clouds around the reference confirms the efficacy of the alignment procedure.

## Discussion

Our findings suggest that different genetic ancestry backgrounds are associated with distinct body types or morphotypes (body shape profiles). For instance, some ancestry sub-samples tend to show greater accumulation of fat in the abdominal area, while others show a more generalized distribution. These differences are not always captured by traditional indicators, which can lead to under- or overestimation of obesity and, consequently, derive into a noisy framework of obesity-related health risks on specific, under-represented populations. Therefore, understanding how body shape varies with ancestry is essential for improving how we define and assess obesity and its associated risks, particularly in admixed populations such as those in Latin America<sup>71</sup>. Indeed, our study demonstrates that in Latin American populations even broad genetic ancestry categories can significantly influence body shape and obesity-related risk stratification.

Clear differences in anthropometric profiles were observed across individuals with different genetic ancestry backgrounds. Notably, waist-based indices (WHR and WHtR) identified a higher proportion of at-risk individuals among those with predominantly Amerindian ancestry, while BMI tended to classify more individuals with predominantly European ancestry as at risk. This supports the hypothesis that universal diagnostic thresholds may inadequately capture obesity-related health risks in admixed populations. These findings align with previous research performed on the *CANDELA* dataset regarding ancestry-linked anthropometric variation<sup>34</sup> and extend them by integrating 3D morphometrics to reveal geometric patterns (e.g., visceral adiposity distribution). These traits are clearly geometric-morphometric aspects of the phenotype that are not captured by traditional indices.

Beyond anthropometric indices, it is important to acknowledge that discrepancies in obesity-related risk classification may become even more pronounced when integrating other clinical and metabolic dimensions, such as biochemical markers (e.g., lipid profile, glucose, insulin), physiological parameters (e.g., blood pressure, resting heart rate), family history of metabolic disease, and lifestyle factors<sup>72,73</sup>. Incorporating these variables alongside ancestry-informed anthropometric and morphometric measures would provide a more comprehensive and personalized assessment of cardiometabolic risk, particularly in genetically heterogeneous populations like those of Latin America [REV-10]<sup>74,75</sup>.

We previously explored the contribution of genomic ancestry and socioeconomic status to obesity in a sample of admixed Latin Americans from the *CANDELA* dataset and reported lack of consistency among indexes when ascertaining obesity<sup>34</sup>. In other words, the proportion of obesity was heavily dependent on the index and the population. We suggested that genomic ancestry has a significant influence on anthropometric measurements, especially on central adiposity, and that better approaches to overweight and obesity phenotypes are needed in order to obtain more precise reference values.

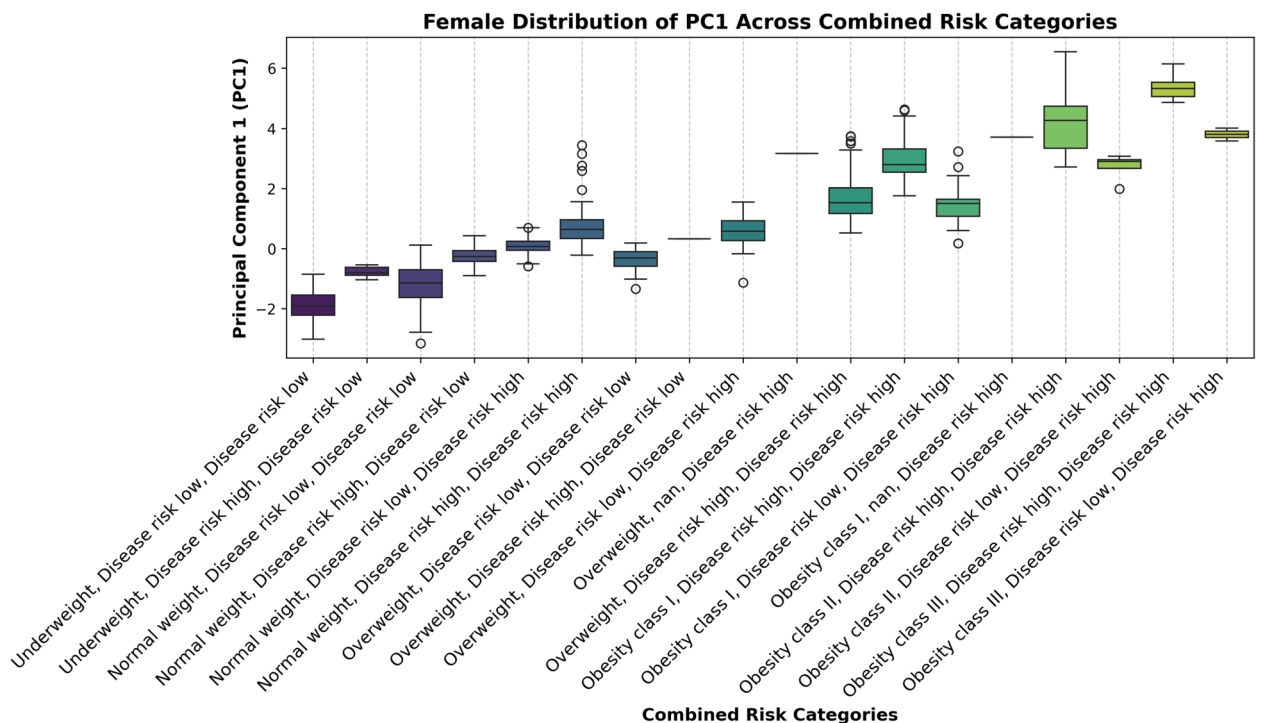


**Fig. 7.** Distribution of Principal Component 1 (PC1) for female participants across combined risk categories defined by BMI, WHR, and WHtR. Each boxplot represents the spread of PC1 scores within a specific category. A progressive increase in PC1 values is observed with increasing levels of obesity and disease risk, suggesting a morphological gradient in body shape associated with cardiometabolic risk profiles.

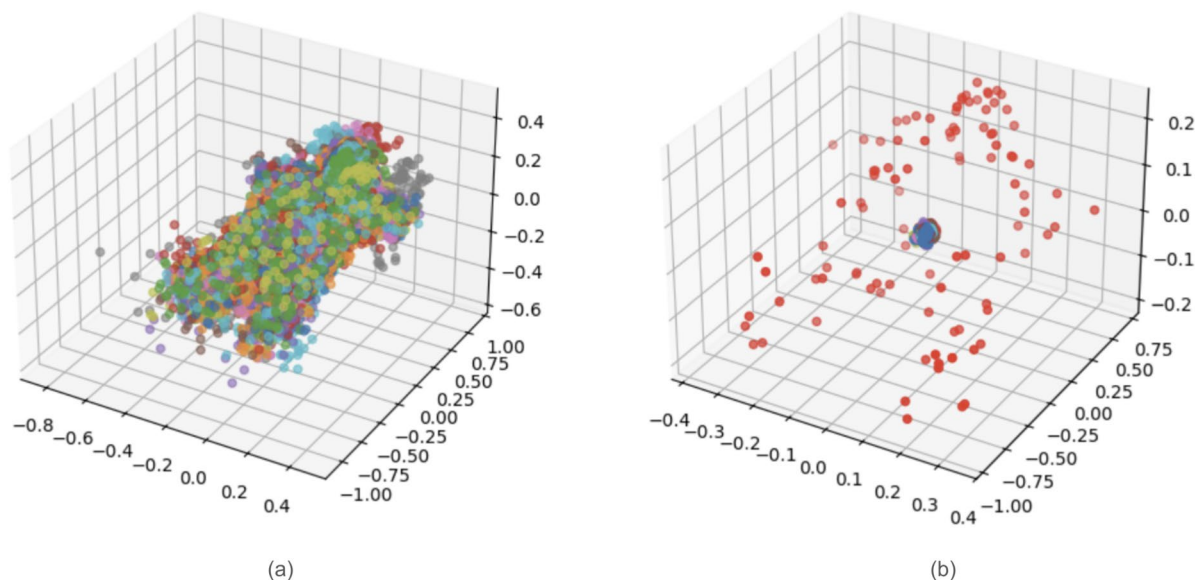


**Fig. 8.** Three-dimensional point distribution of body models before (left) and after (right) Generalized Procrustes Analysis. **(a)** Each color represents an individual model, showing variation in size, orientation, and position. **(b)** After alignment, models are superimposed onto a common reference (red), enabling clearer comparison of shape by eliminating non-shape differences.

In Navarro et al. (2020) we attempted to improve upon classical anthropometric measures of obesity and explored 3D image-based computational approaches to capture the distribution of abdominal adipose tissue as an aspect of shape<sup>35</sup>. We reported shape indicators to be good predictors of the behavior of classical measurements, and evaluated the accuracy of 3D features to describe body shape, overweight and obesity related traits. More recently, we developed more accurate 3D models and representations of body shape, which enabled more precise, systematic, and fast measuring capabilities<sup>43,64</sup>. The shape indicators reported in said papers proved to be accurate predictors of classical indices, adding geometric characteristics that reflect more properly the shape of the bodies under study. This dataset included raw point clouds and parameterized 3D body surfaces, enabling both anthropometric and geometric morphometric analyses. The study demonstrated that 3D-derived shape variables could capture meaningful variation in body morphology and were reliable predictors of traditional anthropometric indices. Importantly, the dataset facilitates the investigation of population-specific body shape patterns, relevant for studying obesity and metabolic health and provides a framework for developing more precise and ancestry-informed phenotypic assessments.

Our team has also propose an automatic 3D body shape-based descriptor and classifier aimed at improving the assessment of obesity beyond traditional anthropometric methods<sup>33</sup>. This computational approach leverages three-dimensional imaging to enable more precise characterization of body shape, particularly in identifying abdominal regions most strongly associated with obesity. By analyzing clustering patterns, the method also allows for the detection of potential risk thresholds, thus supporting large-scale epidemiological studies.

### Ancestry-driven variation in obesity phenotypes

From an evolutionary perspective, the disparities detected here may reflect ancestral adaptations to distinct energetic environments. The thrifty genotype hypothesis<sup>76</sup> posits that alleles promoting efficient fat storage were advantageous in pre-industrial societies with intermittent food scarcity. Such alleles could disproportionately influence central adiposity in Amerindian-descended groups, whose evolutionary history involved extreme climatic and nutritional pressures (e.g., Andean high-altitude adaptations)<sup>77</sup>. Conversely, European ancestry components may be associated with peripheral fat deposition, as seen in our BMI-dominant risk cluster-a pattern potentially linked to colder climate adaptations<sup>78</sup>. However, broad tri-hybrid models need to be further refined to implement more fine-grained ancestry panels that are necessary to detect more local adaptive past processes or drift-derived patterns of variation (e.g. See<sup>25</sup>).

### Pitfalls of one-size-fits-all diagnostics

Our Venn analyses revealed that only 62% of high-risk individuals were concurrently identified by BMI, WHR, and WHtR, with ancestry group-specific disagreement rates (Amerindian: 28%; European: 19%). This inconsistency mirrors critiques of BMI's validity in South Asian and African populations<sup>79,80</sup> and underscores two critical gaps.

These discrepancies highlight two key limitations in current obesity assessment strategies. On the clinical side, an over-reliance on BMI may lead to the underdiagnosis of individuals at metabolic risk, particularly among Amerindian-dominant populations who may present a “healthy” BMI yet show elevated WHtR values indicative of central adiposity. On the methodological side, traditional anthropometric indices are unable to

distinguish between subcutaneous fat, which may be metabolically neutral or protective, and visceral fat, which is strongly associated with adverse health outcomes. This distinction, however, becomes apparent through the application of 3D shape analyses, such as principal component analysis (PCA), which allow for a more precise characterization of body fat distribution. These two gaps are clearly exposed in our analyses of Guatemalan Maya-Kaqchikel cohort (*SER project*), where 34% of women classified as “healthy” by BMI fell into high-risk WHtR categories, echoing disparities observed in Indigenous populations globally<sup>81</sup>. These findings align with Rubino et al. (2025), and support the use of complementary measures alongside BMI to better identify at-risk individuals across diverse ancestries<sup>6</sup>.

### 3D morphometrics: precision and pragmatism

Our Procrustes-based shape analysis represent a formalization of the three-dimensional shape of the human body in our sample, and identified three ancestry-correlated morphotypes. Individuals with predominant Amerindian ancestry tended to exhibit a “centralized” body shape, characterized by higher PC2 scores and a distribution pattern resembling apple-shaped obesity, which is often linked to higher visceral fat accumulation and cardiometabolic risk. In contrast, those with predominant European ancestry displayed a more “diffuse” body shape, with lower PC1 and PC2 scores, corresponding to a gynoid fat distribution typically concentrated around the hips and thighs—an arrangement often considered metabolically less harmful. Admixed individuals, as expected, presented a spectrum of “intermediate” morphotypes, reflecting heterogeneous body shape configurations and risk profiles that do not fit neatly into existing diagnostic categories.

While 3D scanning offers unparalleled resolution, it still needs a scalability strategy in order to achieve a clinical concrete using. Here we propose a two-tiered approach. We propose a two-tiered approach to bridge this gap. In research and clinical settings, high-resolution 3D scanners combined with fine-grained ancestry informative marker (AIM) panels can be employed to refine ancestry-specific thresholds for obesity-related risk assessment. For broader public health applications, more accessible and scalable technologies, such as AI-assisted video morphometry tools like *body2vec\_mesh*<sup>43</sup>, could enable large-scale screening and monitoring of body shape and composition, particularly in under-resourced settings. This dual strategy balances precision with accessibility, advancing the integration of shape-based metrics into both precision medicine and population-level interventions.

### Navigating the ancestry-race-ethnicity triad

Genetic ancestry, as quantified here via AIMs, is a biological construct distinct from the sociopolitical dimensions of race/ethnicity<sup>46</sup>. However, their entanglement in Latin America—where European ancestry often correlates with higher socioeconomic status<sup>23</sup>—demands cautious interpretation. For instance, the elevated obesity risk in our European-dominant group may reflect gene-environment interactions (e.g., urbanized diets) rather than innate biological differences. Future studies should integrate socio-demographic covariates (e.g., income, urbanization) to disentangle genetic and environmental effects, avoiding deterministic narratives<sup>82</sup>.

### Future directions and policy implications

To move toward more equitable and effective strategies for obesity assessment, we highlight three key areas of action. First, ancestry-aware guidelines should be developed by leveraging data from admixed populations to define region-specific obesity thresholds. Mexico’s implementation of WHtR-based standards serves as a valuable precedent in this regard<sup>83</sup>. Second, the democratization of technology is essential to expand access to advanced phenotyping methods. This includes validating low-cost tools, such as smartphone-based 3D scanning, for use in resource-limited settings<sup>36,84–86</sup>. Finally, promoting global health equity requires addressing the stark underrepresentation of Latin American populations in genetic and obesity research. Currently, less than 5% of genomics studies related to obesity include data from this region<sup>87</sup>, limiting the generalizability and applicability of findings in global health contexts. To achieve these goals, it is crucial to increase the collection of high-quality data on obesity, cardiometabolic diseases, and fat distribution, ideally including 3D body composition measures and body shape from all ancestry groups in any given populations. Such data are essential for identifying accurate links between morphotypes and health risks and, in so doing, create novel, ancestry-informed predictors of risk and establishing diagnostic thresholds that reflect the biological diversity of global populations more accurately. Without this foundation, current models risk perpetuating structural biases and diagnostic inaccuracies, particularly in regions with high genetic admixture and limited representation in biomedical research. Moreover, our approach also reinforces the importance of policy engagement, necessary to the implementation of novel methodological approaches aimed to guarantee more sophisticated diagnostic procedures and a broader, more egalitarian access of patients from different socio-economic contexts to it. However, the underlying biological background and fine-grained information must be leveraged responsibly—acknowledging the societal dimensions of health disparities while refining tools to detect them.

### Conclusion

Our findings demonstrate that genetic ancestry is a significant determinant of anthropometric variation and cardiometabolic risk classification in Latin American populations. Across both sexes, BMI, WHR, and WHtR varied systematically by ancestry group, with Native American ancestry consistently associated with higher values for all indices and a greater proportion of individuals classified as high risk. Among these measures, WHR emerged as the most discriminative index, followed closely by WHtR, highlighting their value in capturing ancestry-specific differences in body fat distribution. Analyses based on AIMs revealed clear associations between genetic ancestry and anthropometric indices, whereas country-level comparisons showed no significant variation, underscoring the primacy of genetic ancestry over geopolitical boundaries in shaping body composition. Our analysis also confirms that the ABSI and HI indices are statistically independent of

BMI and height. This independence validates their use as complementary tools for a more accurate assessment of health risk in diverse populations. Additionally, PCA confirmed a consistent morphological gradient across risk categories, with PC1 capturing combined variation in BMI, WHR, and WHtR, and aligning strongly with cardiometabolic risk stratification. Finally, 3D body shape alignment using Generalized Procrustes Analysis proved effective for standardizing models and isolating shape variation, reinforcing the utility of geometric morphometric approaches for refining obesity risk assessment. Collectively, these results highlight both the limitations of applying uniform diagnostic thresholds across admixed populations and the need for ancestry-informed, shape-based criteria to improve the accuracy and equity of cardiometabolic risk evaluation in diverse populations.

### Data availability

Raw genotype or phenotype data cannot be made available due to restrictions imposed by the ethics approval. Summary statistics from previous GWAS on the CANDELA consortium data have been deposited in GWAS central <https://www.gwascentral.org/study/HGVST1841/> and <http://www.gwascentral.org/study/HGVST3308>. The Raíces and Patagonia3D Lab datasets have been deposited in the CONICET Digital Repositorio and can be accessed at <http://hdl.handle.net/11336/161809> and <http://hdl.handle.net/11336/179519>. For the SER project, as participants did not provide unrestricted consent for future unspecified research, access and use of the de-identified datasets used in the current study may be requested from the corresponding author if the focus of the proposed secondary data analysis falls within the original consent provided by participants and the requesting researcher obtains ethics approval for the proposed secondary data analysis from their institutional ethics board. Additional datasets used and analyzed during the current study are available from the corresponding author upon reasonable request.

Received: 7 July 2025; Accepted: 18 September 2025

Published online: 24 October 2025

### References

1. Temple, N. J. The origins of the obesity epidemic in the USA—lessons for today. *Nutrients* **14**, 4253 (2022).
2. Speakman, J. R. The evolution of body fatness: Trading off disease and predation risk. *J. Exp. Biol.* **221**, jeb167254 (2018).
3. Prentice, A. M., Hennig, B. J. & Fulford, A. Evolutionary origins of the obesity epidemic: Natural selection of thrifty genes or genetic drift following predation release?. *Int. J. Obes.* **32**, 1607–1610 (2008).
4. Speakman, J. R. Thrifty genes for obesity, an attractive but flawed idea, and an alternative perspective: The ‘drifty gene’ hypothesis. *Int. J. Obes.* **32**, 1611–1617 (2008).
5. Sohail, M. et al. Mexican biobank advances population and medical genomics of diverse ancestries. *Nature* **622**, 775–783 (2023).
6. Rubino, F. et al. Definition and diagnostic criteria of clinical obesity. *Lancet Diabetes Endocrinol.* (2025).
7. National Institutes of Health. National institute of diabetes and digestive and kidney diseases. Tech. Rep., US Renal Data System, USRDS 1998 Annual Data Report (2010).
8. Waalen, J. The genetics of human obesity. *Transl. Res.* **164**, 293–301 (2014).
9. Marti, A., Moreno-Aliaga, M., Hebebrand, J. & Martinez, J. Genes, lifestyles and obesity. *Int. J. Obes.* **28**, S29–S36 (2004).
10. Comuzzie, A. G. & Allison, D. B. The search for human obesity genes. *Science* **280**, 1374–1377 (1998).
11. Caleyachetty, R. et al. Ethnicity-specific BMI cutoffs for obesity based on type 2 diabetes risk in England: A population-based cohort study. *Lancet Diabetes Endocrinol.* **9**, 419–426 (2021).
12. Montani, J.-P. Ancel keys: The legacy of a giant in physiology, nutrition, and public health. *Obes. Rev.* **22**, e13196 (2021).
13. Bennett, J. P. et al. Three-dimensional optical body shape and features improve prediction of metabolic disease risk in a diverse sample of adults. *Obesity* **30**, 1589–1598 (2022).
14. Thomas, D. M. et al. Updates on methods for body composition analysis: Implications for clinical practice. *Curr. Obes. Rep.* **14**, 8 (2025).
15. Qiao, C. et al. Prediction of total and regional body composition from 3D body shape. *NPJ Digit. Med.* **7**, 298 (2024).
16. Ng, B. K. et al. Detailed 3-dimensional body shape features predict body composition, blood metabolites, and functional strength: The shape up! studies. *Am. J. Clin. Nutr.* **110**, 1316–1326 (2019).
17. Cakir, H., Heus, C., van der Ploeg, T. J. & Houdijk, A. P. Visceral obesity determined by CT scan and outcomes after colorectal surgery; a systematic review and meta-analysis. *Int. J. Colorectal Dis.* **30**, 875–882 (2015).
18. El-Serag, H. B. et al. Visceral abdominal obesity measured by CT scan is associated with an increased risk of Barrett’s oesophagus: A case-control study. *Gut* **63**, 220–229 (2014).
19. Poonawalla, A. H. et al. Adipose tissue MRI for quantitative measurement of central obesity. *J. Magn. Reson. Imaging* **37**, 707–716 (2013).
20. Machann, J., Horstmann, A., Born, M., Hesse, S. & Hirsch, F. W. Diagnostic imaging in obesity. *Best Pract. Res. Clin. Endocrinol. Metab.* **27**, 261–277 (2013).
21. Lingvay, I., Cohen, R. V., Roux, C. W. & Sumithran, P. Obesity in adults. *Lancet* **404**, 972–987 (2024).
22. Salzano, F. M. & Bortolini, M. C. *The Evolution and Genetics of Latin American Populations* (Cambridge University Press, 2002).
23. Adhikari, K., Mendoza-Revilla, J., Chacón-Duque, J. C., Fuentes-Guajardo, M. & Ruiz-Linares, A. Admixture in Latin America. *Curr. Opin. Genet. Dev.* **41**, 106–114 (2016).
24. Adhikari, K., Chacón-Duque, J. C., Mendoza-Revilla, J., Fuentes-Guajardo, M. & Ruiz-Linares, A. The genetic diversity of the Americas. *Annu. Rev. Genomics Hum. Genet.* **18**, 277–296 (2017).
25. Chacón-Duque, J.-C. et al. Latin Americans show wide-spread converso ancestry and imprint of local native ancestry on physical appearance. *Nat. Commun.* **9**, 5388 (2018).
26. Homburger, J. R. et al. Genomic insights into the ancestry and demographic history of South America. *PLoS Genet.* **11**, e1005602 (2015).
27. Li, Q. et al. Automatic landmarking identifies new loci associated with face morphology and implicates Neanderthal introgression in human nasal shape. *Commun. Biol.* **6**, 481 (2023).
28. Peng, F. et al. Genome-wide association studies identify multiple genetic loci influencing eyebrow color variation in Europeans. *J. Invest. Dermatol.* **139**, 1601–1605 (2019).
29. Li, Q. et al. Pitx2 expression and Neanderthal introgression in *hs3t3a1* contribute to variation in tooth dimensions in modern humans. *Curr. Biol.* **35**, 131–144 (2025).
30. Faux, P. et al. Neanderthal introgression in *scn9a* impacts mechanical pain sensitivity. *Commun. Biol.* **6**, 958 (2023).

31. Boekstegers, F. et al. Development and internal validation of a multifactorial risk prediction model for gallbladder cancer in a high-incidence country. *Int. J. Cancer* **153**, 1151–1161 (2023).
32. Zollner, L. et al. Gallbladder cancer risk and indigenous south American mapuche ancestry: Instrumental variable analysis using ancestry-informative markers. *Cancers* **15**, 4033 (2023).
33. Freire-Gómez, C., Paschetta, C., González-José, R., Delrieux, C. et al. Automatic 3d body shape-based classifier: A computational approach to understanding obesity (2025). Manuscript submitted for publication.
34. Ruderman, A. et al. Obesity, genomic ancestry, and socioeconomic variables in latin american mestizos. *Am. J. Hum. Biol.* **31**, e23278 (2019).
35. Navarro, P. et al. Body shape: Implications in the study of obesity and related traits. *Am. J. Hum. Biol.* **32**, e23323 (2020).
36. Trujillo-Jiménez, M. A. et al. Body2vec: 3d point cloud reconstruction for precise anthropometry with handheld devices. *J. Imaging* **6**, 94 (2020).
37. Hünemeier, T. et al. Niger-congo speaking populations and the formation of the brazilian gene pool: mtDNA and y-chromosome data. *Am. J. Phys. Anthropol. Offic. Publ. Am. Assoc. Phys. Anthropol.* **133**, 854–867 (2007).
38. Fejerman, L. et al. Genome-wide association study of breast cancer in latin american identifies novel protective variants on 6q25. *Nat. Commun.* **5**, 5260 (2014).
39. Zavala, V. A. et al. Cancer health disparities in racial/ethnic minorities in the united states. *Br. J. Cancer* **124**, 315–332 (2021).
40. Ruiz-Linares, A. et al. Admixture in Latin America: Geographic structure, phenotypic diversity and self-perception of ancestry based on 7,342 individuals. *PLoS Genet.* **10**, e1004572 (2014).
41. Paschetta, C. et al. Raíces: una experiencia de muestreo patagónico. In *Libro de Resúmenes de las Decimocuartas Jornadas Nacionales de Antropología Biológica*, vol. 1 (In Spanish, 2019).
42. Gasaneo, S. et al. Correlación entre la ansiedad, la depresión, la atención y los hábitos alimentarios. In *XIX Reunión Nacional y VIII Encuentro Internacional de la AACC* (2023).
43. Trujillo Jiménez, M. A. *Reconstrucción antropométrica 3D de bajo costo basada en procesamiento de imágenes y Deep Learning* (Universidad Nacional del Sur, Bahía Blanca, Argentina, 2024).
44. Nepomnaschy, P. A., Welch, K., McConnell, D., Strassmann, B. I. & England, B. G. Stress and female reproductive function: A study of daily variations in cortisol, gonadotrophins, and gonadal steroids in a rural mayan population. *Am. J. Hum. Biol. Offic. J. Hum. Biol. Assoc.* **16**, 523–532 (2004).
45. Barha, C. K. et al. Child mortality, hypothalamic-pituitary-adrenal axis activity and cellular aging in mothers. *PLoS ONE* **12**, e0177869 (2017).
46. Lewis, A. C. et al. Getting genetic ancestry right for science and society. *Science* **376**, 250–252 (2022).
47. Wojcik, G. L. et al. Genetic analyses of diverse populations improves discovery for complex traits. *Nature* **570**, 514–518 (2019).
48. Belbin, G. M. et al. Toward a fine-scale population health monitoring system. *Cell* **184**, 2068–2083 (2021).
49. Rosenthal, E. A. et al. Comparing ancestry standardization approaches for a transancestry colorectal cancer polygenic risk score. *Genet. Epidemiol.* **49**, e22590 (2025).
50. Paschou, P., Lewis, J., Javed, A. & Drineas, P. Ancestry informative markers for fine-scale individual assignment to worldwide populations. *J. Med. Genet.* **47**, 835–847 (2010).
51. Cerqueira, C. C. et al. Implications of the admixture process in skin color molecular assessment. *PLoS ONE* **9**, e96886 (2014).
52. World Health Organization. *Waist Circumference and Waist-Hip Ratio* (Tech. Rep. Report of a WHO Expert Consultation, 2008).
53. Umuerr, E. M. Ethnicity and cut-off values in obesity. In *Nutrition in the Prevention and Treatment of Abdominal Obesity* (ed. Umuerr, E. M.) 211–223 (Elsevier, 2019).
54. Consultation, W. Waist circumference and waist-hip ratio. *Report of a WHO Expert Consultation. Geneva: World Health Organization* **2008**, 8–11 (2008).
55. Huxley, R., Mendis, S., Zheleznyakov, E., Reddy, S. & Chan, J. Body mass index, waist circumference and waist: Hip ratio as predictors of cardiovascular risk—a review of the literature. *Eur. J. Clin. Nutr.* **64**, 16–22 (2010).
56. McKnight, P. E. & Najab, J. Kruskal-wallis test. *The corsini encyclopedia of psychology* 1–1 (2010).
57. Dunn, O. J. Multiple comparisons using rank sums. *Technometrics* **6**, 241–252 (1964).
58. Krakauer, N. Y. & Krakauer, J. C. Dynamic association of mortality hazard with body shape. *PLoS ONE* **9**, e88793 (2014).
59. Krakauer, N. Y. & Krakauer, J. C. A new body shape index predicts mortality hazard independently of body mass index. *PLoS ONE* **7**, e39504 (2012).
60. Krakauer, N. Y. & Krakauer, J. C. An anthropometric risk index based on combining height, weight, waist, and hip measurements. *J. Obes.* **2016**, 8094275 (2016).
61. Krakauer, N. Y. & Krakauer, J. C. Novel anthropometric indices: An allometric perspective. *Endocrines* **6**, 44 (2025).
62. Mendoza-Revilla, J. et al. Disentangling signatures of selection before and after European colonization in Latin Americans. *Mol. Biol. Evol.* **39**, msac076 (2022).
63. Kramer, O. & Kramer, O. Scikit-learn. *Machine Learning for Evolution Strategies* 45–53 (2016).
64. Trujillo-Jiménez, M. A. et al. 3dpatbody: 3d dataset of human bodies of a patagonian population and their anthropometric measurements. *Sci. Data* **11**, 1360 (2024).
65. Osokin, D. Real-time 2d multi-person pose estimation on cpu: Lightweight openpose. arXiv preprint [arXiv:1811.12004](https://arxiv.org/abs/1811.12004) (2018).
66. Saito, S., Simon, T., Saragih, J. & Joo, H. Pifuhd: Multi-level pixel-aligned implicit function for high-resolution 3d human digitization. In: *Proc. IEEE/CVF conference on computer vision and pattern recognition*, 84–93 (2020).
67. Slice, D. E. Geometric morphometrics. *Annu. Rev. Anthropol.* **36**, 261–281 (2007).
68. Mitteroecker, P., Gunz, P., Windhager, S. & Schaefer, K. A brief review of shape, form, and allometry in geometric morphometrics, with applications to human facial morphology. *Hystrix Ital. J. Mammal.* **24**, 59–66 (2013).
69. Virtanen, P. et al. Scipy 1.0: Fundamental algorithms for scientific computing in python. *Nat. Methods* **17**, 261–272 (2020).
70. Zhou, Q.-Y., Park, J. & Koltun, V. Open3d: A modern library for 3d data processing. arXiv preprint [arXiv:1801.09847](https://arxiv.org/abs/1801.09847) (2018).
71. Fernández-Rhodes, L. et al. A gene-accluturation study of obesity among us hispanic/latinos: The hispanic community health study/study of latinos. *Psychosom. Med.* **85**, 358–365 (2023).
72. Amirabdollahian, F. & Haghghatdoost, F. Anthropometric indicators of adiposity related to body weight and body shape as cardiometabolic risk predictors in british young adults: superiority of waist-to-height ratio. *J. Obesity* **2018**, 8370304 (2018).
73. Piché, M.-E., Tchernof, A. & Després, J.-P. Obesity phenotypes, diabetes, and cardiovascular diseases. *Circ. Res.* **126**, 1477–1500 (2020).
74. Alberti, K. G. M., Zimmet, P. & Shaw, J. The metabolic syndrome—a new worldwide definition. *Lancet* **366**, 1059–1062 (2005).
75. Manolopoulos, K., Karpe, F. & Frayn, K. Gluteofemoral body fat as a determinant of metabolic health. *Int. J. Obes.* **34**, 949–959 (2010).
76. Neel, J. V. Diabetes mellitus: A ‘thrifty’ genotype rendered detrimental by ‘progress’?. *Am. J. Hum. Genet.* **14**, 353–362 (1962).
77. Bigham, A. W. et al. Identifying positive selection candidate loci for high-altitude adaptation in andean populations. *Hum. Genomics* **4**, 79–90. <https://doi.org/10.1186/1479-7364-4-2-79> (2009).
78. van der Lans, A. A. et al. Cold acclimation recruits human brown fat and increases nonshivering thermogenesis. *J. Clin. Investig.* **123**, 3395–3403 (2013).
79. Nuttall, F. Q. Body mass index: Obesity, bmi, and health: A critical review. *Nutr. Today* **50**, 117–128. <https://doi.org/10.1097/NT.000000000000092> (2015).

80. Sekgala, M. D., Sewpaul, R., Opperman, M. & Mchiza, Z. J. Comparison of the ability of anthropometric indices to predict the risk of diabetes mellitus in south African males: Sanhanes-1. *Int. J. Environ. Res. Public Health* **19**, 3224 (2022).
81. Anderson, I. et al. Indigenous and tribal peoples' health (the lancet-lowitja institute global collaboration): A population study. *Lancet* **388**, 131–157 (2016).
82. Borrell, L. N. et al. Race and genetic ancestry in medicine—a time for reckoning with racism (2021).
83. Abúndez, C. O. et al. Encuesta nacional de salud y nutrición 2006. *Instituto Nacional de Salud Pública* (2006).
84. Lim, H.-w. & Jafari, R. Exploration in 3d body scanning mobile applications. In: *Proc. 4th International Conference in Emotion and Sensibility: Convergence of AI and Emotional Science. Korean Society for Emotion and Sensibility* (2021).
85. Stark, E., Haffner, O. & Kučera, E. Low-cost method for 3d body measurement based on photogrammetry using smartphone. *Electronics* **11**, 1048 (2022).
86. Foyosal, K. H., Chang, H.-J., Bruess, F. & Chong, J.-W. Body size measurement using a smartphone. *Electronics* **10**, 1338 (2021).
87. Popejoy, A. B. & Fullerton, S. M. Genomics is failing on diversity. *Nature* **538**, 161–164 (2016).

## Acknowledgements

For the support and data supply, the authors would like to express deep thanks to the *CANDELA Consortium*, *Raices*, *Patagonia3DLab*, *ECHA* and *SER* projects.

## Author contributions

M.A.T.-J., P.N, C.D. and R.G.-J. conceived the original idea. M.C.B., V.A.-A., S.C.-Q., G.P., C.G., F.R., W.R., A.R.-L. and R.G.-J. made the *CANDELA Consortium* data collection. M.A.T.-J., L.O.P., C.P., V.R., A.R., M.U., P.T.-M., L.M., C.F.-G., P.Na., S.D.A., B.P., T.T. and R.G.-J. made the *Raices and Patagonia3DLab* collection of data. M.A.T.-J., S.G. and G.G. made the *ECHA* data collection. M.A.T.-J., A.R., and P.N made the *SER Project* collection of data. M.A.T.-J., P.N, C.D. and R.G.-J. conducted the experiments and analysed the results. M.A.T.-J., P.N, C.D. and R.G.-J. wrote the manuscript. All authors have read and agreed to the published version of the manuscript.

## Declarations

### Competing interests

The authors declare no competing interests.

### Additional information

**Supplementary Information** The online version contains supplementary material available at <https://doi.org/10.1038/s41598-025-21071-w>.

**Correspondence** and requests for materials should be addressed to M.A.T.-J.

**Reprints and permissions information** is available at [www.nature.com/reprints](http://www.nature.com/reprints).

**Publisher's note** Springer Nature remains neutral with regard to jurisdictional claims in published maps and institutional affiliations.

**Open Access** This article is licensed under a Creative Commons Attribution-NonCommercial-NoDerivatives 4.0 International License, which permits any non-commercial use, sharing, distribution and reproduction in any medium or format, as long as you give appropriate credit to the original author(s) and the source, provide a link to the Creative Commons licence, and indicate if you modified the licensed material. You do not have permission under this licence to share adapted material derived from this article or parts of it. The images or other third party material in this article are included in the article's Creative Commons licence, unless indicated otherwise in a credit line to the material. If material is not included in the article's Creative Commons licence and your intended use is not permitted by statutory regulation or exceeds the permitted use, you will need to obtain permission directly from the copyright holder. To view a copy of this licence, visit <http://creativecommons.org/licenses/by-nc-nd/4.0/>.

© The Author(s) 2025